Effect of Structural Dynamics on the Shaft Line Rotor Response in Turbomachines

E. Meli, G. Pallini, A. Rindi, F. Capanni and S. Rossin

Abstract The accurate model of the complicated dynamic phenomena characterizing rotors and support structure represents a critical issue in the rotor dynamic field. A correct prediction of the whole system behavior is fundamental to identify safe operating conditions and to avoid instability operating range that may lead to erroneous project solutions or possible unwanted consequences for the plant. Although a generic rotating machinery is mainly composed by four components (rotors, bearings, stator and supporting structure), many research activities are often more focused on the single components rather than on the whole system. The importance of a combined analysis of rotors and elastic supporting structures arises with the continuous development of turbomachinery applications, in particular in the Oil and Gas field where a wide variety of solutions, such as off-shore installations or modularized turbo-compression and turbo-generator trains, requires a more complete analysis not only limited to the rotor-bearing system. Complex elastic systems such as rotating machinery supporting structures and steel foundations might, in some situations, strongly dominate the entire shaft line rotor dynamic response (mode shapes, resonance frequencies and unbalance response). They give birth to transfer functions which will introduce coupling phenomena between machines bearings, becoming enablers of a new shaft line dynamic. Since FEM theory offers a number of different solutions to represent the rotor and the

E. Meli (✉) · G. Pallini · A. Rindi
Industrial Engineering, University of Florence, Florence, Italy
e-mail: enrico.meli@unifi.it

G. Pallini
e-mail: giovanni.pallini@unifi.it

A. Rindi
e-mail: andrea.rindi@unifi.it

F. Capanni · S. Rossin
Auxiliary Systems Engineering, GE Oil and Gas, Florence, Italy
e-mail: francesco.capanni@ge.com

S. Rossin
e-mail: stefano.rossin@ge.com

J.K. Sinha (ed.), *Vibration Engineering and Technology of Machinery*,
Mechanisms and Machine Science 23, DOI 10.1007/978-3-319-09918-7_87

rotating machine support system (beam models, solid models, transfer function, etc.), in this paper a great emphasis is given to the results of an experimental campaign done on a centrifugal compressor as validation of the new rotor dynamic approach.

Keywords Rotating machines · Shaft line · Structural dynamics · Dynamics stiffness · Bearings · Dynamic interaction

1 Introduction

This research activity aims to study how baseplates cause coupling transfer functions [1] between different bearings and the unavoidable need of the inclusion of this component in the analysis since project preliminary stages. There is clearly a limitation in the simplification of the supporting structure model and its effect on the dynamic of the system. As visible in Eq. (1), in the transfer function *Tf* the cross talking terms (K_{12}, K_{21}) link the DOFs of different bearings, as reported on Fig. 1, effecting the final dynamic response of the system.

$$Tf = \begin{bmatrix} K_{11} & K_{12} \\ K_{21} & K_{22} \end{bmatrix} \tag{1}$$

The appearance of cross talk terms deeply modify the response of the rotor [2, 5, 6], if compared to the classical approaches where $K_{12} \equiv K_{21} \equiv 0$ and the direct terms K_{11} and K_{22} act as a series of springs with the characteristic of bearings. In particular the influence of cross talk terms become more interesting in the second rocking or flexible mode of the rotor that is typical of the off-shore installation due to the isostatic anchoring system and to the deck flexibility.

The integration of the supporting structure dynamics may lead to the following:

- The system response highlights the modes of each individual component of the assembly;

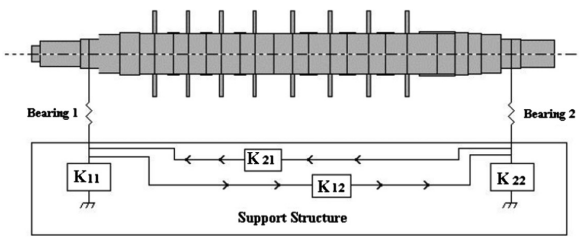

Fig. 1 Direct and cross talk terms

- The rotor modes shift in frequency without modification of the deformed shapes;
- The rotor keeps almost constant modes frequency but with different shapes.

As mentioned in [3], when the stiffness ratio $K_{support}/K_{brg} \leq 3.5$, the support flexibility begins to have a significant influence on the system's critical speeds and response characteristics. Such ratio is clearly a guideline to guarantee a good behaviour in the operating range; however the structural dynamic response is way from being constant in the machine speed range and a more deep characterization may be needed.

The general architecture (see Fig. 2) of this study highlights the mutual interaction between the three main components: rotor, bearings and support. The flow of local variables (forces, torques and kinematic variables) shows the primary importance of bearings as filter element interposed between the baseplate and the rotor. Bearings will be modelled as equivalent spring-damper, dependent on the running speed.

Two steps are required to accomplish the analysis: *the first step* considers the rotor mounted directly on foundations and there will not be any sort of model simplification; *the second step* leads to the reduction of calculation time instead, introducing assumption to represent the supporting structure in a simplified way. A scheme of the general architecture is visible in Fig. 2.

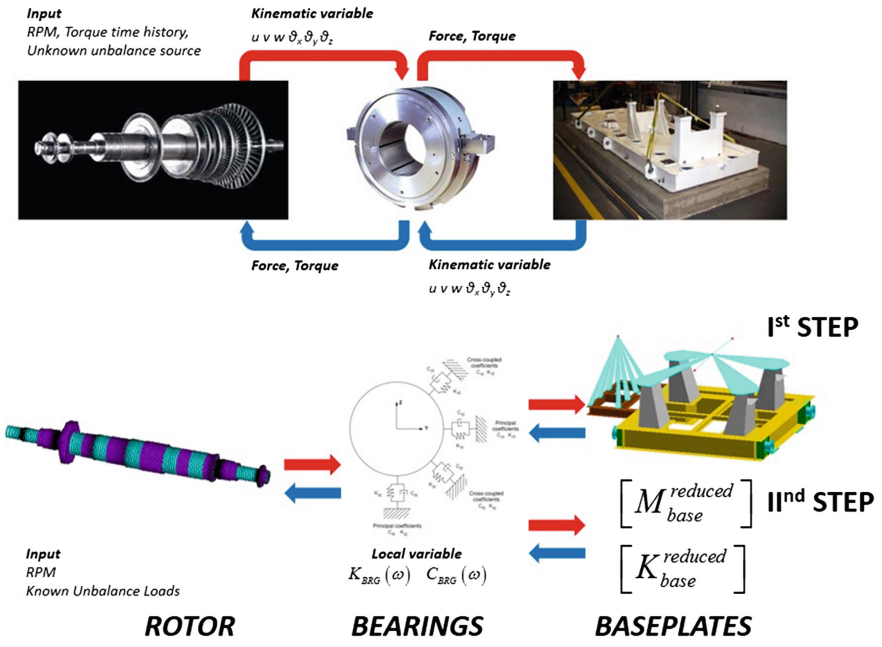

Fig. 2 General architecture

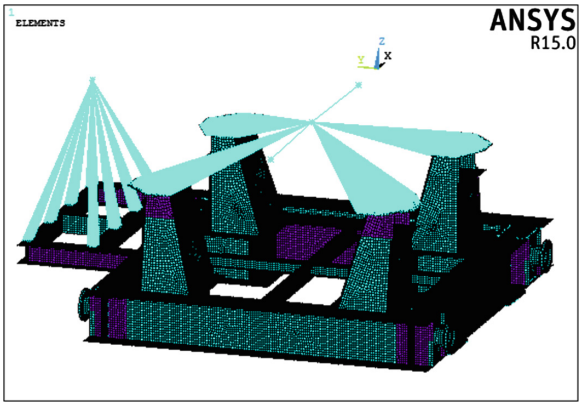

Fig. 3 FEM elastic support structure

The calculation time reduction is strictly related to the use of Craig–Bampton Component Mode Synthesis technique [4] that generally can be considered an extension of the Guyan and modal reduction techniques.

The model in the first step is implemented using one of the most common FEM software, Ansys (Fig. 3), and then in the second phase is compared with XLTRC^2, a software fully dedicated to the rotordynamic field. To consider the dynamic contribution of the support structure, XLTRC^2 make use of the Mass and Stiffness reduced matrix as outcome of the Ansys CMS procedure.

This document highlights the correspondence between the rotor dynamic numerical investigation and experimental data acquisition on a machine start up high vibration issue experienced on a five stage MCL centrifugal compressor.

2 The Model

I Step: In the first step of the analysis the elements (rotor and support structure) are fully described considering six degrees of freedom and no simplification have been performed to reduce the dimension of the mathematical problem to solve.

The main component of the assembly is the rotor shaft. The rotor is the sum of many contributions and it must take into account the effect of the keyed and shrink fitted elements. The representation of the impeller simulate the increasing in mass due to the extra component and to properly describe the dynamics of the real part it includes concentrated mass and inertia features suitably distributed along the length of the shaft.

The resulting equation that describes the rotor is:

$$\begin{aligned}&\left\{\left[M_{shaft}\right]+\left[M_{sleeve}\right]+\left[M_{mi}\right]\right\}\left\{\ddot{q}_{rotor}\right\}\\&\quad+\left\{\left[C_{shaft}\right]+\Omega\left[G_{shaft}\right]+\Omega\left[G_{mi}\right]\right\}\left\{\dot{q}_{rotor}\right\}+\left[K_{shaft}\right]\left\{q_{rotor}\right\}=F\end{aligned}\tag{2}$$

where M_{shaft}, K_{shaft}, C_{shaft}, G_{shaft} respectively specifies the naked rotor mass, stiffness, damping and gyroscopic effect matrix, M_{sleeve} indicate the mass contribution of shrink fitted elements (like impeller), M_{mi} and G_{mi} explicit the dynamic contribute (concentrated properties m_x, m_y, m_z, I_p, I_t) of elements modelled as sleeves, then F represent external forces.

The F_y and F_z forces that the bearings exert on the rotor can be expressed in terms of linearized force coefficients for small perturbations about a stationary equilibrium at a given shaft speed. The forces are expanded as follows:

$$\{F_{BRG}\} = \begin{Bmatrix} F_y \\ F_z \end{Bmatrix} = \begin{bmatrix} -K_{yy} & -K_{yz} \\ -K_{zy} & -K_{zz} \end{bmatrix} \begin{Bmatrix} y \\ z \end{Bmatrix} + \begin{bmatrix} -C_{yy} & -C_{yz} \\ -C_{zy} & -C_{zz} \end{bmatrix} \begin{Bmatrix} \dot{y} \\ \dot{z} \end{Bmatrix} \tag{3}$$

where K_{yy}, K_{zz} and C_{yy}, C_{zz} are *Direct stiffness and damping coefficients*, while K_{yz}, K_{zy}, C_{yz}, C_{zy} represent the *Cross-coupling stiffness and damping coefficients.*

The entire baseplate, is bounded to the ground with spring element. The spring stiffness is extracted from dynamic stiffness simulations to satisfy the results of hammer test on the supporting pedestals.

Assembling the equations of the full system, Eq. (4), so introducing the effects of supports, the new set of coordinate $\{q\} = \{q_{rot}, q_{base}\}^T$ correspond to a rearrangement of the vector containing the coordinate of the node related to the rotor $\{q_{rot}\}$ and to the support structure $\{q_{base}\}$

$$\begin{aligned} &\{[M_{rotor}] + [M_{base}]\}\{\ddot{q}\} + \{[C_{rotor}] + [C_{base}] + \Omega[G_{rotor}]\}\{\dot{q}\} \\ &\quad + \{[K_{rotor}] + [K_{base}]\}\{q\} = F_{BRG} + F^{ext} \end{aligned} \tag{4}$$

II Step: The second step doesn't introduce any change to the rotor model.

The baseplate is the sum of different elements: *shell* to model the steel structure, *rigid connections* to represent joints and describe the casing, *concentrated mass and inertia properties* for the contribution of the centrifugal compressor casing to the assembly dynamic and *spring* to model the effect of the ground.

In the second step of the analysis a modal reduction of the baseplate (*fixed interface CMS*) has been performed to extract the reduced mass and stiffness matrices necessary to introduce the dynamic contribute of the supporting structure in XLTRC^2.

Master DOFs have been chosen on the boundary of the support structure and the result of this consideration tells that nodes that perfectly suit the circumstances are, as highlighted in Fig. 4 Master node location nodes on the extremity of elements that represent the linking between bearings and foundations. Acronyms DE and NDE, used to mark the left and right end, come from the original system where you can recognize the location of the torque input and actually DE means Drive End and NDE stand for Non Drive End.

As the goal of this analysis is to describe the flex-torsional behavior of the assembly each master node (located at the bearing interface) considers all the six DOFs (three rotations and three translations).

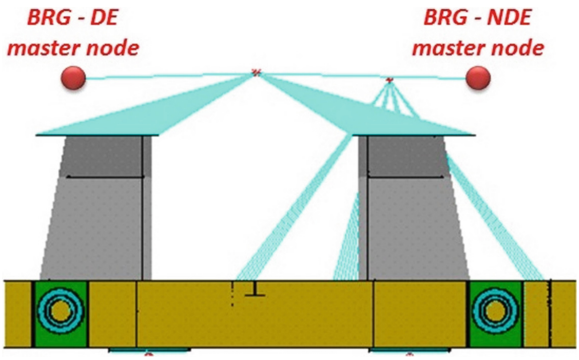

Fig. 4 Master node location

Considering the equation of the whole system, by this time the coordinate vector contains the reduced coordinate of the baseplate $\{q_{red}\} = \{q_{rotor}, q_{base}^{red}\}^T$ and so the complete equation of the system turns into:

$$\begin{aligned}&\left\{[M_{rotor}] + \left[M_{base}^{red}\right]\right\}\{\ddot{q}_{red}\} + \left\{[C_{rotor}] + \left[C_{base}^{red}\right] + \Omega[G_{rotor}]\right\}\{\dot{q}_{red}\} \\ &\quad + \left\{[K_{rotor}] + \left[K_{base}^{red}\right]\right\}\{q_{red}\} = F_{brg} + F^{ext}\end{aligned} \tag{5}$$

The biggest disadvantage of CMS approach is the increase of the problem size if compared to the matrices used with Static and Modal reduction. Furthermore CMS provides dense matrices, neither diagonal, like modal reduction outputs, nor sparse, as the original model. Despite all troubles, Craig–Bumpton's method guarantees excellent results with non-optimal master nodes distribution as well as in case of a poor modal base, furthermore it gives great benefits for the reduction of calculation time and matrices are always smaller than the original problem.

In general the fixed interface CMS considers only a subset of the constrained eigenmodes and the dimension of the matrix depends on a frequency band chosen by the user $[0,\omega_{max}]$ that is a function of the frequency domain to investigate.

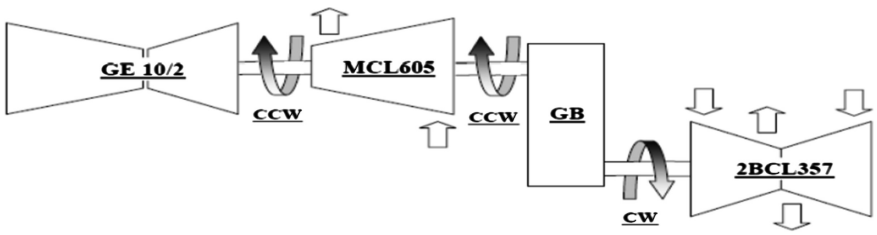

Fig. 5 Rotor train

3 Experimental Data: Turbo Compression Train

As result of a high shaft vibration issue on a centrifugal compressor experienced on field, a great number of vibration data have been gathered on both structure and proximity probes.

The compression system was made up of a gas turbine with two centrifugal compressors and one gearbox in one single shaft line (Fig. 5). Each rotating machine was installed on a separate baseplate steel structure and the individual rotors were connected by elastic coupling.

High vibration was detected at the proximity probes of both bearings at one of the two compressors, compromising anyway the proper train start up sequence. From the preliminary data acquisition on structure vibration reviled an unexpected response close to the operating speed but not to the extent to justify the train trip shut down.

Solution to the problem was the insertion of concrete underneath the baseplate to redefine a suitable anchoring system.

Several seismic probes were positioned at the compressor pedestals (Fig. 6 Seismic probes arrangement, steel baseplate structure and compressor casing, measuring vibration level along the horizontal and vertical directions (amplitude and phase)).

The structure mode shapes and frequencies were retrieved from a sequence of machine start up and shut down by means of a dedicated post processing procedure called Operating Modal Analysis (OMA). The extracted modes shape and frequencies were then compared to the one computed by dedicated FE models with the purpose of verification and subsequent model tuning.

Due to the complexity of the mechanical system under investigation and the strong focus on the effect of the structural dynamics on the overall shaft dynamics, a great accuracy of the baseplate FE model was fundamental for a robust experimental and numerical system validation.

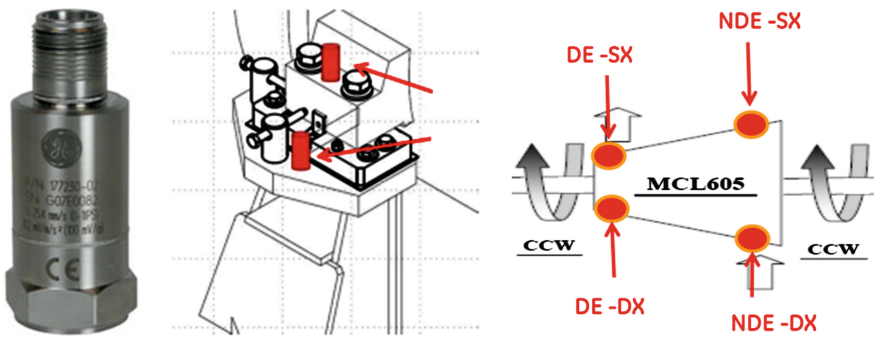

Fig. 6 Seismic probes arrangement

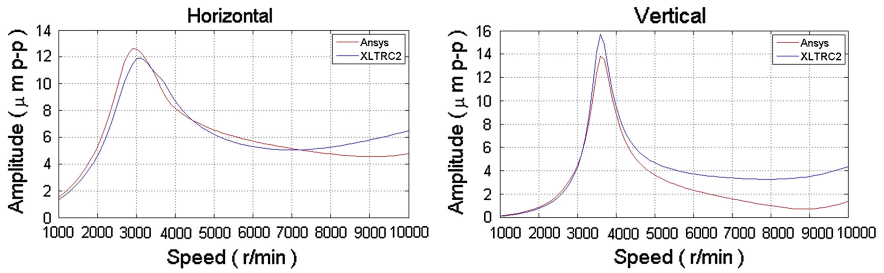

Fig. 7 Amplitude absolute displacements, first mode, only rotor, non drive end

4 Results and Major Findings

The amplitude of the synchronous unbalance U used for the system response is described in Eq. (6). According to the API standard the equation below represents the load to be applied at the location of maximum displacement, that to stimulate the first deformed shape corresponds to the bearings mid span

$$U = 4[6350(W/N)] \; [gmm] \tag{6}$$

where N represents the maximum continuous operating speed in *rpm* and W is the journal static weight load in kilograms.

Comparing the results obtained from both modelling software (Ansys and XLTRC^2) the response of the rotor without the support structure flexibility is revealing a strong match in the vicinity of the first shaft resonance mode (Fig. 7).

Even though one can appreciate the good match on the first rotor mode frequency (critical speed) there is still a substantial deviation for high frequencies as well as between vertical and horizontal directions.

Taking a close look to the dynamic stiffness of the supporting structure and comparing that with both the bearing stiffness and the limit identified from API617 as 3.5 times the bearings stiffness it is possible to see that indeed the structure on its own shows a degrading stiffness for shaft speed lower than the maximum operating speed. In Fig. 8 the areas below the bearing stiffness indicate a lack of stiffness along the vertical direction and so a potential "critical speed range".

When the support structure is included in the whole mechanical system, the overall picture of the shaft unbalance response drastically changes. The first shaft mode slightly shifts towards the high frequencies and the structural modes emphasize themselves as shaft response. Once again in the next picture (Fig. 9) the comparison of the models implemented in Ansys and XLTRC^2 underlines the good match between the two models after the introduction of the support system dynamics.

As the proximity probes measure a relative displacement between the compressor casing and the shaft, a proper post processing need to be done for a better

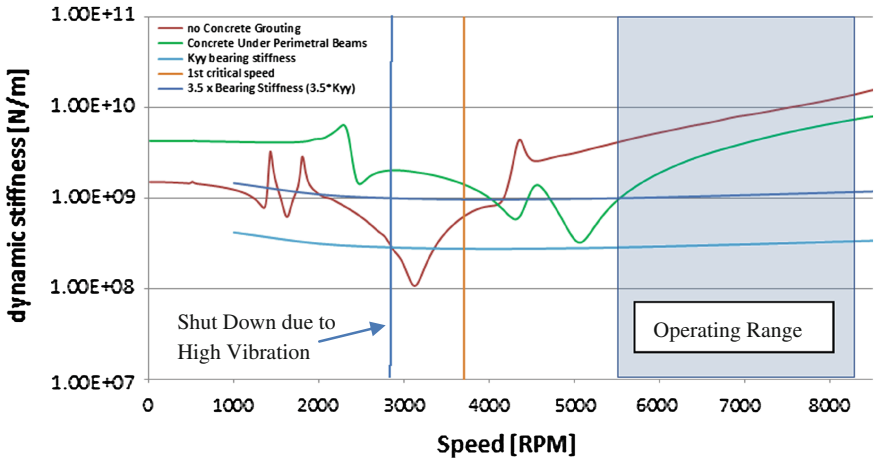

Fig. 8 Dynamic stiffness in vertical direction

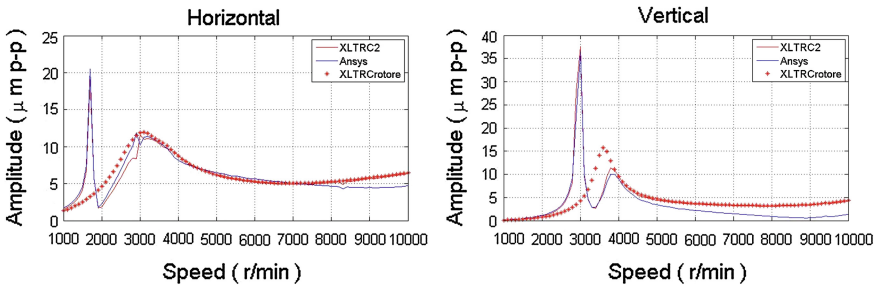

Fig. 9 Absolute displacements—rotor at bearing station

comparison with the experimental data (Fig. 11 relative displacements response of the system before and after concrete reinforcement).

The introduction of the concrete under the supporting structure produces a shift of the structural resonance (highlighted in the experimental test at 3,000 rpm) and this can be clearly seen on both the computational (Fig. 11) and experimental results (Fig. 10).

The response of the complete mechanical system with and without the additional concrete grouting (*grouting*—contraction *GR*) is overlaid to the dynamic response of the rotor alone (Fig. 11) understanding how much the study of the rotor in "stand alone" condition can deceive a rotordynamic study.

Looking at the grouting versus no grouting shaft response (Fig. 12 right column) the evidence of the strong benefit on the critical behavior at 3,000 rpm is clear. The proximity probe measurement retrieved after the additional concrete grouting (Fig. 12 left column) is in strong agreement with the final computational results even in sharp peak at pure structural response.

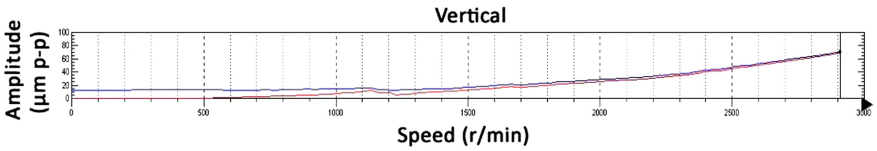

Fig. 10 Run up shut down condition: exceeded vibration level

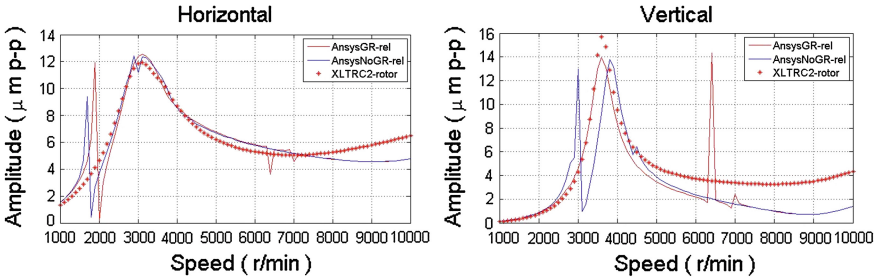

Fig. 11 Relative displacements response of the system before and after concrete reinforcement

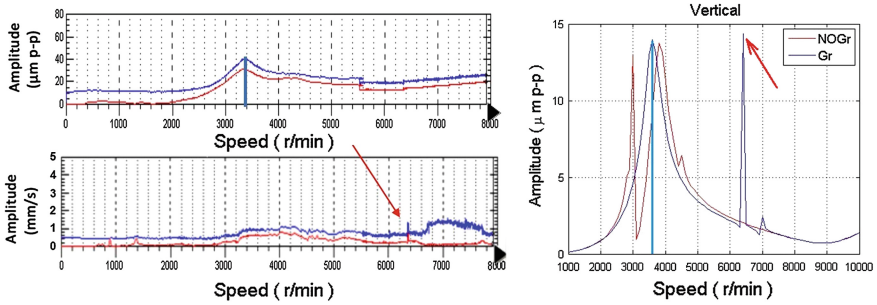

Fig. 12 Comparison between simulated (*right column*) relative displacements and experimental (*left column*) data

5 Conclusions

The behavior of a Rotor machine is not simple to predict and many tools and theories need to be compared at the same time to have a complete vision of the real behavior.

It is not sufficient to evaluate the different component of the rotating machine separately, it is important to have a deep knowledge of the entire assembly behavior (rotor, bearing and support structure) to predict the mutual influence of design parameter and allow different parallel working team to elaborate the problem with the right input.

The model, oriented in creating an accurate tool for the rotor dynamic of the whole machine, is at the moment a good improvement in terms of time and accuracy.

A future development is the representation of a complete train shaft line with experimental match out of dedicated experimental data.

Acknowledgment A special thanks to Valentina Peselli from Enginsoft s.r.l. for managing a thorough FE model debugging, finding the appropriate element selection within Ansys model, helping the team to find the pitfall of some element formulation which could not otherwise drive us to the result validation.

References

1. Cuppens K, Sas P, Hermans L (2000) Evaluation of the FRF based substructuring and modal sinthesis technique applied to vehicle FE data
2. Vazquez J, Barrett L (1999) Transfer function representation of flexible supports and casings of rotating machinary. In: IMAC-XVII-17th international modal analysis conference 1999
3. API Pubblication 684 (1996) Tutorial on the API standard paragraphs covering rotor dynamics and balancing: an introduction to lateral critical and train torsional analysis and rotor balancing
4. Bampton MCC, Craig RR (1968) Coupling of substructures for dynamic analysis. AIAA J 6 (7):1968
5. Kruger T, Liberatore S, Knopf E (2013) Complex substructures and their impact on rotor dynamic. In: SIRM 2013—10th international conference on vibrations in rotating machines, 2013
6. Ehehalt U, Luneburg B, Daniel C, Strackeljan J, Woschke E (2009) Methods to incorporate foundation elasticities in rotordynamic calculation. In: SIRM 2009—8th international conference on vibrations in rotating machines, 2009